Development of Better Quality Low-Cost Activated Carbon from South African Pine Tree (*Pinus patula*) Sawdust: Characterization and Comparative Phenol Adsorption

L. Mukosha, M. S. Onyango, A. Ochieng, and H. Kasaini

Abstract—The remediation of water resources pollution in developing countries requires the application of alternative sustainable cheaper and efficient end-of-pipe wastewater treatment technologies. The feasibility of use of South African cheap and abundant pine tree (*Pinus patula*) sawdust for development of low-cost AC of comparable quality to expensive commercial ACs in the abatement of water pollution was investigated. AC was developed at optimized two-stage N_2-superheated steam activation conditions in a fixed bed reactor, and characterized for proximate and ultimate properties, N_2-BET surface area, pore size distribution, SEM, pH_{PZC} and FTIR. The sawdust pyrolysis activation energy was evaluated by TGA. Results indicated that the chars prepared at 800°C and 2hrs were suitable for development of better quality AC at 800°C and 47% burn-off having BET surface area (1086m^2/g), micropore volume (0.26cm^3/g), and mesopore volume (0.43cm^3/g) comparable to expensive commercial ACs, and suitable for water contaminants removal. The developed AC showed basic surface functionality at pH_{PZC} at 10.3, and a phenol adsorption capacity that was higher than that of commercial Norit (RO 0.8) AC. Thus, it is feasible to develop better quality low-cost AC from (*Pinus patula*) sawdust using two-stage N_2-steam activation in fixed-bed reactor.

Keywords—Activated carbon, phenol adsorption, sawdust integrated utilization, economical wastewater treatment.

I. INTRODUCTION

THE numerous public health problems which have plagued many regions of developing countries are as a result of lack of safe drinking water due to poor management of water resources [1]. Water is a fundamental natural resource and indispensable to life. The rapid industrialization and massive urbanization of rapid growing human population are the cause of increased amounts and types of toxic chemical pollutants loading to receiving water bodies [2], [3]. The embracing of industrialization as integral to economic and social developments of the country must be accompanied with strict

L. Mukosha is with the Chemical Engineering Department, Copperbelt University, Kitwe, P. O. Box 21692, Zambia (phone: +260 968 999068; fax: +260 212 228212; e-mail: loimwimba@yahoo.com).

M. S. Onyango is with the Chemical and Metallurgy Department, Tshwane University of Technology, Pretoria, Private Bag X680, South Africa (phone: +27 23823533; Fax: +27 123823532; e-mail: OnyangoMS@tut.ac.za).

A. Ochieng is with the Chemical Engineering Department, Vaal University of Technology, Vanderbijlpark 1900, South Africa (phone: +27 (0) 16950 9884; Fax: +27 (0) 16 950 9796; e-mail: ochienga@vut.ac.za).

H. Kasaini is with the Rare Element Resources Corporation, Denver, USA (e-mail: henry_kasaini@yahoo.com).

environmental pollution control measures. It is well known that mining, metallurgical and chemical industries constitute the largest fraction of principal point sources of toxic chemicals (metal ions and organic chemicals) in water bodies. Therefore, the effective and efficient control of the level of toxic chemicals at the point of industrial effluent discharge is a critical step in the chain of water resources pollution control. However, the consistent achieving of regulatory wastewater discharge limits for toxic water contaminants requires application of efficient end-of-pipe wastewater treatment technologies. The conventional wastewater treatment technology of chemical precipitation has problems of incomplete precipitation, inability to remove dissolved metal complexes [4], and inefficient in removal of amphoteric hydroxides [5] and dissolved toxic organic molecules [3]. Also, the precipitation removal of toxic chemicals generates voluminous toxic sludge to which disposal is an environmental problem. The conventional biological treatment is inefficient in removal of toxic soluble organic chemicals due to toxicity inhibitory effect on the active microbes and/or the organic chemicals could be recalcitrant or not readily biodegradable [6], [7]. On the other hand, the available advanced wastewater treatment technologies e.g. reverse osmosis, ion exchange, advanced oxidation, [commercial] activated carbon adsorption, solvent extraction, etc are expensive to implement and maintain in developing countries [8]. Nevertheless, the adsorption technology with utility of low-cost adsorbents is highly feasible for efficient and economical remediation of water resources pollution in developing countries.

In the context of South Africa (SA) an opportunity gap exists in the integrated utilization of sawdust waste from an invasive pine tree (*Pinus patula*). Despite sawdust utilization in the form of sawdust pellets, biomass boiler feed, power generation at demonstration stage [9], there is still an estimated 6 million tons/year of sawdust going to actual wastage [10] i.e. simply open air sawdust incineration without energy capture or otherwise to reduce pile volumes at sawmills. The wasted sawdust provides a practical and sustainable source for development of better quality low-cost AC for efficient abatement of toxic metal ions and organic chemicals from industrial and municipal wastewaters at reduced cost.

World Academy of Science, Engineering and Technology
International Journal of Chemical and Molecular Engineering
Vol:7, No:7, 2013

The aim of this study was to evaluate the feasibility of developing low-cost AC of textural quality and aqueous phase phenol removal capacity comparable to expensive commercial ACs. Water resources pollution by phenol is a concern worldwide due to phenol high toxicity to aquatic organisms and humans even at low concentrations in water bodies [11]. Phenol health effects on humans include damages to lungs, kidneys and liver. The major sources of phenol in water bodies are wastewater discharges from a large number of industries that include phenolic resins, oil refinary and petrochemicals, coal gasification, pesticides, textiles, disinfectants, fertilizers, etc. The widely used technology for removal of phenol from wastewater is the biological treatment [7]. However, this technology is inefficient for phenol removal due toxicity inhibitory effect on active microbes. Therefore, there is need to research for alternative efficient and cheaper technology for phenol removal from wastewaters. There is scant literature on the use of South Africa pine tree (*Pinus patula*) sawdust for development of better quality low-cost AC of high phenol adsorption capacity comparable to expensive commercial ACs. This study focused on optimization of carbonization and activation process conditions of superheated steam activation method in fixed-bed reactor for development of sawdust low-cost AC of high surface area, pore volume, pore size distribution, and surface functionalities suitable for aqueous phase application. The equilibrium adsorption capacity for phenol of the developed low-cost AC was compared to that of commercial AC (Norit RO 0.8).

II. MATERIALS AND METHODS

Large quantities of sawdust from South Africa pine tree (*Pinus patula*) go to waste. There is an opportunity to utilize this wasted sawdust for development of better quality low-cost AC for efficient removal of toxic pollutants in wastewaters at reduced cost. The AC samples were developed from sawdust by the 2-stage N_2-superheated steam activation.

A. Materials

The AC precursor material used in this study was South Africa pine tree (*Pinus patula*) sawdust obtained locally (Singisi sawmill, KwaZulu Natal, SA). The properties of the sawdust are shown in Table I. The nitrogen gas (99.99%) was purchased from Afrox, SA. NaOH, HCl and NaCl were purchased from SMM, SA. Commercial AC, Norit RO 0.8 (Sigma, USA) was used for comparative phenol (99+%, SMM, SA) adsorption capacities with the developed low-cost AC. All the chemicals used were of analytical grade.

B. Sawdust Pyrolysis Characteristics and Kinetics

The sawdust pyrolysis characteristics and kinetics were studied using thermal gravimetric Analysis (TGA, Perkin Elmer) in the temperature range 25-900°C for evaluation of the carbonization temperatures to effect extensive devolatilization of the sawdust. The lumped (primary and secondary pyrolysis zones) apparent activation energy of the sawdust was estimated by fitting the TGA data to the nth order reaction Arrhenius pyrolysis model [12]:

$$\ln\left(\frac{d\alpha}{dT}\right) - n\ln(1-\alpha) = \ln\left(\frac{A}{\text{Б}}\right) - \frac{E_a}{RT} \tag{1}$$

$$\alpha = (m_i - m(t))/(m_i - m_f)$$

$$d\alpha/dT = (\alpha_{T2} - \alpha_{T1})/(T2 - T1); \quad = dT/dt$$

where, α is the conversion (fraction of pyrolyzed biomass) with m_i, m_t and m_f the masses (g) of biomass at the beginning, time t and the end of the TGA event respectively; T is the absolute temperature (K); dα/dT is the pyrolysis rate (K^{-1}); n is the pyrolysis reaction order; A is the pre-exponential factor; Б is the heating rate (K/min); E_a is the slow pyrolysis activation energy (kJ/mol^2) and R is the universal gas constant (8.314kJ/mol).

C. Preparation of Activated Carbon

The experimental setup for the fixed-bed carbonization and activation of the sawdust was shown in Fig. 1. The sawdust was sieved to obtain a particle size fraction of –4+2mm, washed with distilled water to remove water soluble impurities and surface adhered particles, and oven dried at 110°C for 24 hrs. Carbonization and activation were done in the same stainless steel vertical tubular reactor (Internal Diameter 38mm, and Length 214mm) heated externally in a tube furnace (Ultra-Furn, UF/UT 12/50/300, SA) equipped with programmable temperature controller. About 30g (Precisa XB220A, Switzerland) of sawdust was carbonized under nitrogen flow (570ml/min N_2) at heat ramp (10K/min) from room temperature to varied final temperatures for common 2hrs residence time, and cooled to room temperature under nitrogen flow. About 15g of char sample(s) of optimally developed initial porosity was heat ramped at 10K/min under 180°C preheated 570ml/min N_2 to 800°C and activated with superheated steam (180°C, 1.6bar, and 780ml/min) for varied residence times of 0.5, 1.0, 1.5, and 2.0hrs. At the end of activation time, the nitrogen preheater was switched off and the AC sample cooled to room temperature under nitrogen flow. The superheated steam was generated from distilled water heated in a laboratory furnace. Prior to start of carbonization and activation processes, the sample loaded reactor was purged off atmospheric oxygen with N_2 gas for 30min.

The char yield (Y_C), AC burn-off (BO) and AC yields (Y_{AC}) were calculated using (2), (3), and (4) respectively.

$$Y_C(\%) = [m_C/m_S]100 \tag{2}$$

$$BO(\%) = [(m_C - m_{AC})/m_C]100 \tag{3}$$

$$Y_{AC}(\%) = [m_{AC}/m_S]100 \tag{4}$$

where, m_C, m_S, and m_{AC} are the masses (g) of sawdust char, sawdust and activated carbon respectively.

World Academy of Science, Engineering and Technology
International Journal of Chemical and Molecular Engineering
Vol:7, No:7, 2013

1. Stainless steel reactor 2. Tubular furnace
3. Steam reheater 4. Water tank
5. steam generator 6. Piston pump
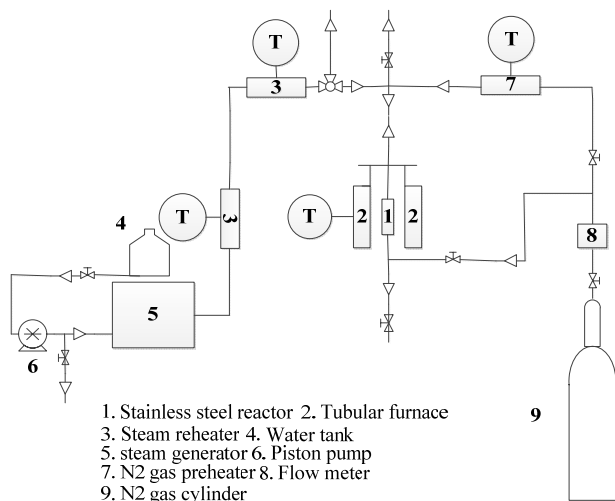7. N2 gas preheater 8. Flow meter
9. N2 gas cylinder

Fig. 1 Carbonization and activation experimental setup

D. Characterization of Carbon Samples

1. Physical, Textural and Morphological Properties

The carbon sample(s) moisture and volatile matter (VM) contents were determined from Thermo gravimetric analysis (TGA, Perkin Elmer) in temperature range 25-900°C [13]. The followed TGA protocol was 25±5mg sample, 20ml/min N_2, 10K/min from 25 - 110°C, 50K/min from 110 - 900°C and 10min hold at 110 and 900°C. The ash content of carbon sample(s) was determined by the ASTM D2866-94 method [14]. The ultimate analysis of the carbon sample(s) was obtained from the CHNS elemental analyser (Elementar vario EL III). The sawdust and char samples textual properties were evaluated by CO_2 adsorption at 273K using ASAP 2020 V3.01 (Micromeritics). Prior to analysis the sawdust and char samples were outgassed at 110°C and 360°C respectively for 24hours. The outgassed (360°C and 24hrs) AC samples textual properties were evaluated by N_2 adsorption at 77K using TriStar II 3020 V1.02 (Micromeritics). The surface morphology of outgassed (150°C and 24hrs) carbon sample(s) was analysed using scanning electron microscope (SEM, Cambridge Instrument 360). The bulk density of AC sample was determined using a graduated volumetric column.

2. Activated Carbon Surface Functionalities

The aqueous suspension pH of oven outgassed (150°C, 24hrs) carbon sample (<45μm) was determined by the ASTM D 3838-80 reflux method [14]. Solution pH was measured using the Orion 4 star, pH meter, USA. The acidity and basicity of AC sample(s) ware determined by the standardized Boehm titration [15]. 250 mg carbon sample added to 15ml solutions of either (0.05M) NaOH or HCl sample bottle and the mixer equilibrated in a thermostated water shaker (Labcom, Maraisburg) at 25°C, 200rpm and 48hrs. In acidity measurements filtrates were back titrated under continuous N_2 gas bubbling with 0.05M NaOH using phenolphthalein indicator. Following the same procedure, the basicity of the filtrate sample was measured by direct titration with 0.05M NaOH. The Infra Red spectrum of oven outgassed (150°C and 24hrs) AC powder sample was acquired by the Nujol paste

method using a Nicolet Impact 410 FTIR spectrometer in the frequency 600 – 4000 cm^{-1} at 4cm^{-1} resolution. The pH of point of zero charge (pH$_{pzc}$) of AC sample(s) was determined by the batch potentiometric method [16]. 25ml of 0.01M NaCl background electrolyte solution was placed in several sample bottles and solutions pH was adjusted between 2 – 11 by addition of known titrant volumes (0.1 – 5ml) of either 0.01M HCl or 0.01M NaOH. N_2 gas was bubbled into each solution to dispel dissolved CO_2 and after pH stabilization initial pH values were recorded. About 75mg (< 45μm) of carbon sample was then added into each bottle, sealed and equilibrated at 25°C, 200rpm, and 48hrs. The final pH of AC suspension(s) was measured. The titration data was treated to obtain the proton binding isotherm [16]:

$$Q = \frac{V_B+V_T}{m}\left[(a_{H^+})_i - (a_{OH^-})_i - (a_{H^+})_f + (a_{OH^-})_f\right] \quad (5)$$

where, Q is the proton consumption (mmol/g), V_B and V_T are volumes (ml) of background electrolyte and titrant respectively, m is the mass of carbon sample (g); $(a_{H^+})_{i, f}$ and $(a_{OH^-})_{i, f}$ are the initial and/or final activities of hydrogen and hydroxyl ions. The initial and final proton activity was calculated from measured pH using the activity coefficient correction from the Davies equation. Activity of hydroxyl ion was obtained from the ionic product of water.

E. Comparative Equilibrium Adsorption

The effect of solution pH on phenol adsorption on developed AC was studied over a pH range 2-12 with 0.8g/l AC and 25ml solutions of 100mg/l phenol at 25°C, 200rpm and 24hrs equilibration. Solutions pH was adjusted using HCl and NaOH solutions. The filtrates equilibrium phenol concentrations was determined using double beam UV-Vis spectrophotometer (Heλios α, Japan) at wavelength of 270nm. The adsorption isotherm of phenol on developed AC and/or Norit AC was obtained at the optimum solution pH, 0.8g/l AC and -300+150μm in a series of sample bottles containing 25ml solution of known phenol concentrations at 25°C, 200rpm, and 24hrs equilibration. The ACs equilibrium phenol uptake was calculated from the mass balance:

$$q_e = [(C_O - C_e)V_S/m_{AC}] \quad (6)$$

where, qe is equilibrium phenol uptake of adsorbent (mg/L), C_O is the initial phenol concentration (mg/L), C_e is the equilibrium phenol concentration in aqueous solution (mg/L), V_S is the volume of solution (L) and m_{AC} is as previously defined. The isotherm data were fitted to the Langmuir and Freundlich isotherm models.

1. Langmuir Isotherm Model [17]:

$$\frac{q_e}{Q_{max}} = \frac{K_L C_e}{1+K_L C_e} \quad (7)$$

$$R_L = \frac{1}{1+K_L C_O} \quad (8)$$

World Academy of Science, Engineering and Technology
International Journal of Chemical and Molecular Engineering
Vol:7, No:7, 2013

where, Q_{max} is the monolayer adsorption capacity (mg/g), K_L is the Langmuir constant related net enthalpy of adsorption (L/mg) and R_L is the dimensionless separation factor: $0 < R_L < 1$ for favourable adsorption; $R_L > 1$ for unfavourable adsorption; $R_L = 1$ for linear adsorption and $R_L = 0$ for irreversible adsorption.

2. Freundlich Isotherm Model [17]:

$$q_e = K_F(C_e)^{Fr} \qquad (9)$$

where, K_F is Freundlich constant related to the adsorption capacity (mg/g) and Fr is the constant related to adsorption intensity or heterogeneous factor: $Fr < 1$ for favourable adsorption and $Fr > 1$ for unfavourable adsorption.

III. RESULTS AND DISCUSSION

The incineration of the abundant sawdust from pine tree in South Africa is prominent. The incineration of sawdust has an opportunity cost of efficient and effective remediation of water resources pollution. In this study, sawdust chars and derived low-cost AC samples are characterized for textural properties to evaluate optimum carbonization/activation process conditions and suitability for the removal of toxic phenol from aqueous solution.

A. Sawdust Properties and Slow Pyrolysis Characteristics

TABLE I
PROXIMATE AND ULTIMATE ANALYSES OF SAWDUST MATERIAL

Sample	Proximate analysis (wt. % dry basis)			Ultimate analysis (wt. %)				
	VM	FC[a]	Ash	C	H	S	N	O[a]
Sawdust	85	15	0.1	51	6	0.1	-	43

a=by difference

Table I shows the proximate and ultimate analyses of South Africa Pine tree (*Pinus patula*) sawdust material. The high volatile matter (VM) and carbon (C), and low ash contents qualify the sawdust for generation of activated carbons through carbonization and activation processes. The low sulphur (S) content of the sawdust is important for environmental pollution of sulphur compounds during ACs preparation. The nitrogen (N) content was below the limit of detect of the employed elemental analyzer.

The non-isothermal TGA and DTG thermographs of the sawdust pyrolysis characteristics were shown in Fig. 2. Sawdust is a non-graphitizable woody lignocellulosic biomass of pyrolytic decomposition stages of dehydration, fragmentation and aromatization (i.e. formation of graphene layers) [18]. The defective nature of graphene layers imparts porosity in chars and ACs. The evaluation of the pyrolysis characteristics of sawdust was important in determining the required carbonization temperatures to effect extensive devolatilization and, therefore, maximizing the development of initial porosity in char samples. The DTG small peak (about 100°C) in temperature range (50 - 150°C) accounted for loss of physically bound moisture, and the actual devolatilization

of sawdust was in the temperature range (200 - 650°C) with maxima volatiles release around 400°C. The completed pyrolytic decomposition of lignocellulose constituents were reported to occur in overlapping temperature ranges; hemicelluloses (210 - 325°C), cellulose (310 - 400°C) and lignin (160 - 900°C) [12]. Therefore, the carbonization of sawdust beyond 400°C progressively increased the lignin content of chars i.e. polyaromatic (graphene) structure of chars. In this study, therefore, temperatures $\geq 600°C$ were selected for extensive devolatilization of sawdust material in the carbonization process.
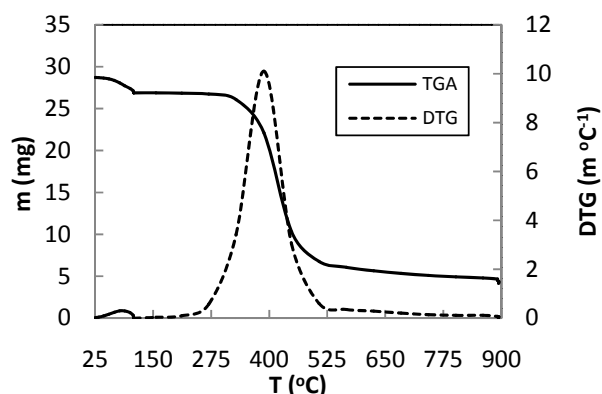

Fig. 2 TGA/DTG curves of sawdust (*Pinus patula*): 20ml/min N₂; 10K/min from 25 to 110°C; 50K/min from 110 to 900°C; 10min hold at 110°C and 900°C; 25mg; -150+70μm

The knowledge of Pine tree (*Pinus patula*) sawdust pyrolysis characteristics and kinetics is also significant for optimal design and control of the carbonization unit for sawdust chars preparation [12], [19]. The devolatilization temperature range (200-400°C) is the primary/active sawdust pyrolysis zone and temperatures > 400°C (i.e. secondary pyrolysis zone) merely increased char aromaticity [19]. The sawdust DTG decomposition data in the temperature range (200-650°C) and α (0.1-0.9) was used to estimate the lumped apparent pyrolysis activation energy through plotting of the nth order reaction Arrhenius pyrolysis model (refer to (1)), and results presented in Fig. 3. In the Arrhenius plot the value of the reaction order 'n' was obtained by trial and error to maximize the linear correlation coefficient (R^2) as shown in Fig. 4. The data fit at n = 1.2 gave maximum $R^2 = 0.980$, and the estimated lumped apparent activation energy and pre-exponential factor were $E_a = 131$kJ/mol and log $P_O = 10$/min respectively. The estimated slow pyrolysis activation energy of (*Pinus patula*) sawdust was in fair agreement with values of biomass slow pyrolysis apparent activation energies reported in literature [14], [19].
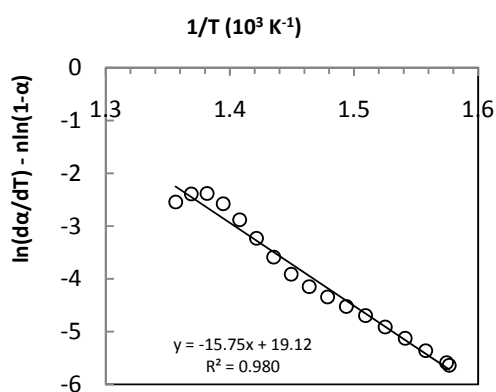
World Academy of Science, Engineering and Technology
International Journal of Chemical and Molecular Engineering
Vol:7, No:7, 2013

Fig. 3 Plot of Arrhenius pyrolysis kinetics model: 476-923K; α (0.1-0.9)
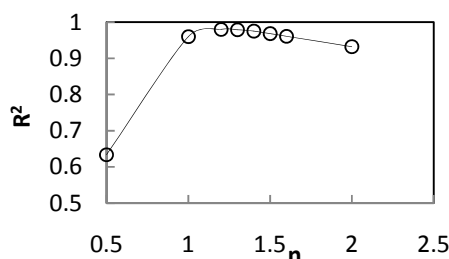

Fig. 4 Iterative estimation of pyrolysis reaction order, n

B. Physical Properties of Sawdust Chars

The sawdust chars were developed by the process of carbonization. Carbonization or slow pyrolysis involves devolatilization of a carbonaceous source material in an inert atmosphere, and thereby imparting initial porosity in the resultant chars. The interest in the carbonization experiments was to maximize the initial porosity of char(s) for subsequent highly porous ACs preparation. Therefore, no attempt of collection and analysis of pyrolytic evolved volatile gases, vapours and tar were made. From the results of the sawdust pyrolysis characteristics, high carbonization temperatures $\geq$ 600°C were used to achieve extensive devolatilization of the sawdust material. Slow heating rate of 10K/min was used in order to develop microporous chars of high initial surface area [20]. High heating rates would reduce the heat transfer resistance in the particle, and hence rapid evolution of volatiles leading to creation of macroporous chars of low initial surface area. In the carbonization of sawdust (*Pinus patula*) in this study, we observed high generation of condensable volatiles and tar. For quick sweep of tar vapours before they could condense and block the reactor gas outlet tube, a relatively high N_2 gas flow rate of 570ml/min was employed. The employed N_2 flow rate was arrived at from a practical balance between rate of N_2 gas consumption and level of tar removal to prevent blockage of reactor gas outlet tube. Reference [21] found negligible effect of inert gas flow rate on char yield for particle sizes $\geq$ 425μm. Therefore, in this study, the evolutions of char physicochemical properties were evaluated at three carbonization temperatures (600, 700, and 800°C) at common heating rate (10K/min) and 2hrs residence time. The developed sawdust chars were denoted by the carbonization temperature, °C/carbonization time, hrs. The results of proximate and ultimate analyses of the sawdust derived chars were presented in Table II.

TABLE II
PROXIMATE, ULTIMATE AND YIELD CHARACTERISTICS OF SAWDUST CHARS

Sample	Proximate analysis (wt. % dry basis)			Ultimate analysis (wt. %)					Yield (%)
	VM	FCa	Ash	C	H	S	N	Oa	
C600/2	18.4	81.2	0.5	70	2.7	0.1	-	27	22
C700/2	15.6	83.9	0.6	75	1.6	0.1	-	23	21
C800/2	13.4	85.4	1.2	77	1.3	0.1	-	21	20

a=by difference

The results of Table II showed trends of decrease in VM, hydrogen (H), S, and oxygen (O) contents, and yield of the chars with increase of carbonization temperature. The char yield minimally decreased with increase of carbonization temperature. The char yields were very low due to the high VM content of the sawdust. Consequently, the fixed carbon (FC) and ash contents of the chars increased with increased of carbonization temperature. The losses of VM and H contents were significant between sawdust and chars, whereas at high temperatures (i.e. 700 and 800°C) the loss of VM and H contents between chars was gradual. The significant decreases in VM content of sawdust resulted in significant increases in FC and ash contents of chars. The increase of FC content was gradual in chars, whereas ash content appreciably increased among chars. The O content greatly decreased between sawdust and chars, but the decrease was gradual between 700 and 800°C. On the other hand the C content greatly increased between sawdust and chars, and appreciably increased among chars, indicative of increased char aromatization with increase of carbonization temperature. The S content was always very low. The decrease in char yield was marginal at high carbonization temperatures. The results seemed to indicate that there could be no significant change of char aromatization for increase of carbonization temperature (>800°C) and/or residence time (>2hrs). In related studies, micropore coalescence or plastic deformation of biomass char samples at high carbonization temperature (> 800°C) was reported [20]. Therefore, in this study, carbonization >800°C and/or > 2hrs residence time was not attempted.

The evolution of chars' porosity/surface area was evaluated by 273K CO_2 adsorption isotherms. The porosity in chars/AC is classified as micropore (<2nm), mesopores (> 2 <50nm) and macropore (>50nm) [18]. The CO_2 adsorption at 273K and P/P_o < 0.03 is confined to measurement of narrow micropores (<0.5nm). Nevertheless, the CO_2 adsorption isotherm data provided a means to compare porosity evolution in chars with increase of carbonization temperature. The results of CO_2 adsorption isotherms of sawdust and sawdust chars were summarized in Table III.

World Academy of Science, Engineering and Technology
International Journal of Chemical and Molecular Engineering
Vol:7, No:7, 2013

TABLE III
SUMMARY REPORT OF CO_2 ADSORPTION ISOTHERMS AT 273K AND $P/P_o <$ 0.03 OF SAWDUST AND DEVELOPED SAWDUST CHARS

Sample	S_{mic} (m^2g^{-1})	V_{mic} (m^3g^{-1} STP)	D_{mic} (nm)
Sawdust	34.05	-	-
C600/2	382.31	0.10	0.37
C700/2	453.46	0.11	0.36
C800/2	485.58	0.13	0.35

S_{mic} = D-R micropore area; V_{mic} = HK micropore volume; D_{mic} = HK ave. pore diameter.

Besides very low surface area of sawdust (*Pinus patula*) material, we observed that the sawdust had the problem of tannin leach into water giving brown-yellow coloration. Similar result of water coloration by sawdust (*Shorea robusta*) material was reported [22]. Therefore, there is need to treat and/or activate sawdust material before application in water/wastewater treatment. The CO_2 adsorption results of sawdust chars showed a general trend of increase of Smic of chars with increase of carbonization temperature. The increase of Smic was significant between sawdust and chars at all temperatures. With increase of carbonization temperature, the Smic reached a higher value at 800°C. However, the increase in Smic was greater in 600-700°C than 700-800°C temperature ranges. The increase in Vmic was minimal in the carbonization temperature range 600-800°C, and the opposite was the case for Dmic. The increase of Smic and V_{mic}, and decrease of D_{mic} with increase of carbonization temperature was indicative of progressive development of microporosity in chars. Similar results were reported [23]. For the carbonization conditions of this study, the chars prepared at 800°C and 2hrs (designated C800/2) developed the highest initial microporosity and were selected as optimal for further porosity/surface area development in the superheated steam activation process.

B. Physical Properties of Activated Carbon Samples

TABLE IV
PROXIMATE AND ULTIMATE ANALYSES AND BURN-OFF AND YIELD OF DEVELOPED ACTIVATED CARBON SAMPLES

Sample	Proximate analysis (wt% db)			Ultimate analysis (wt %)					Yield (%)
	VM	FC[a]	Ash	C	H	S	N	O[a]	
A800/0.5	14.0	84.8	1.9	76	1.2	-	-	22.8	17
A800/1.0	14.8	83.0	2.3	75	1.1	-	-	23.9	14
A800/1.5	15.7	81.2	3.0	74	1.0	-	-	25.0	10
A800/2.0	16.0	80.8	3.2	73	1.0	-	-	26.0	6

a= by difference

Table IV shows the results of proximate and ultimate analyses of AC samples developed from chars developed at the optimum carbonization conditions of 800°C and 2hrs. The AC samples were prepared by steam activation i.e. partial gasification of chars with superheated steam at 800°C and varied activation times (0.5-2.0hrs) corresponding to burn-offs (17-62%). The activation temperature employed to develop the AC samples was same as the carbonization temperature (800°C) of chars. Since the activation times (0.5–2.0hrs) were not higher than the chars carbonization time (2hrs), the

changes in the composition of AC samples were attributed [only] to degree of burn-off. The results of proximate and ultimate analyses showed trends of decrease in FC, C, and H contents of AC samples with increase in burn-off. The VM, Ash, and O contents increased with increase of activation time/burn-off. The S and N contents were below limit of detection of the analysis instrument. These results are to be expected since the steam gasification reactions selectively remove active carbons and/or heteroatoms at graphene edges and defect sites, and enhancement of carbon-oxygen surface groups [18]. The VM of the samples could be attributed to decomposition of carbon-oxygen surface groups. The decrease of C and H contents were gradual with increase of burn-off, whereas it was the opposite for O content. With increase of carbon burn-off the FC decreased causing appreciable increase in ash content. The decrease in AC yield (17–6%) was significant for any increase of activation time (0.5–2.0hrs).

The evolution of the prepared AC samples textural properties with burn-off were evaluated by the 77K N_2-adsorption/desorption isotherms and results presented in Table V.

TABLE V
SUMMARY REPORT OF 77K N_2-ADSORPTION/DESORPTION ISOTHERMS OF DEVELOPED ACTIVATED CARBON SAMPLES

Sample	BO (%)	S_{BET} m^2g^{-1}	S_{mic} (m^2g^{-1})	V_T (cm^3g^{-1})	V_{mic} [cm^3g^{-1} (%)]	D_{ave} (nm)
A800/0.5	17	567	412	0.28	0.19(67.04)	2.0
A800/1.0	30	715	435	0.41	0.20 (48.78)	2.3
A800/1.5	47	1086	576	0.69	0.26 (37.68)	2.5
A800/2.0	62	848	436	0.55	0.20(36.36)	2.6

S_{BET}: BET surface area; S_{mic}: t-plot micropore area; V_T: total pore volume; V_{mic}: t-plot wide micropore volume; D_{ave}: BET average adsorption pore diameter.

The results in Table V showed trends of increase of AC samples textural properties with increase of activation time upto 47% burn-off. At 62% burn-off the textural properties were lower than at 47% burn-off indicating that the textural properties peaked with increase of burn-off. For burn-off ≤ 47%, the increase of activation time increased S_{BET}, S_{mic}, V_T, V_{mic} and $D_{(ave)}$ of AC samples. The mesopre volume can be calculated as difference of V_T and V_{mic}. Bracketed values in V_{mic} column indicate percentage amount. We noticed that the increase of wide micropores volume with increase of activation time was accompanied with a decrease of amount (%) of wide micropores in samples. Accordingly, therefore, the increase of mesopore volume (i.e. $V_T − V_{mic}$) of samples with increase of activation time was accompanied with increase of amount (%) of mesopores in the samples. These results indicated that besides creation of more micropores and mesopores with increase of activation time, portions of exisiting micropores were being widened to mesopores. However, the increase of burn-off to 62% resulted in micropore collapse i.e. excessive widening of micropre to mesopores and/or macropores, and mesopores to macropores. Therefore, the S_{BET}, Smic, V_T, and V_{mic} at 62% burn-off were lower than at 47% burn-off. Consequently, the V_{meso} and D_{ave}

World Academy of Science, Engineering and Technology
International Journal of Chemical and Molecular Engineering
Vol:7, No:7, 2013

were higher at 62% burn-off than at 47% burn-off. The existance of maxima in AC surface area evolution with burn-off was similarly reported [24]. High AC surface area/microporosity is desirable on account of highest adsorption energy of micropores. However, in aqueous phase adsorption narrow microporosity would be closed to solute molecules of rather large molecular/ionic sizes [18], [25]. Therefore, in aqueous phase applications, ACs of high wide microporosity ($> 0.5 < 2$nm) and proportion of mesoporosity ($> 2 < 50$nm) are desirable for rapid entrance of adsorptive molecules to adsorption sites. At low concentrations of solutes as found in wastewater/water treatment, wide micropores are sites of higher adsorption energies and, mesopores of lower adsorption energies function as conduits for adsorptives to interior wide micropores. Under the experimental conditions of this study, the AC sample developed at activation temperature 800°C and 1.5hrs (denoted A800/1.5) developed the highest apparent surface area (1086m^2/g), wide micropore volume (0.26cm^3/g), and mesopore volume (0.43cm^3/g) suitable for aqueous phase application. Therefore, the steam activation conditions of 800°C and 1.5hrs (47% bur-off), together with the other process conditions of this study, were selected as optimal for development of low-cost AC suitable for wastewater treatment. Though the overall AC yield at 47% burn-off was rather low at 10%, the AC production economics are still encouraging because of the bulk availability of cheap sawdust which has limited economic and environmental utilization options.

The SEM micrographs of sawdust, C800/2 chars and AC samples were shown in Fig 5. The carbonization and activation processes developed pseudomorphor structures of the sawdust i.e. the sawdust structure was preserved. However, the carbonization process developed surface pores that seem to have closed in the C800/2 chars. The seeming pore closure could be attributed to surface condensation of some internally devolatilized tars in the sawdust. Nevertheless, the steam gasification/activation process opened up and developed more surface pores in the C800/2 chars. The micrographs revealed no discernible trend in morphological changes of AC samples with increase of activation time.
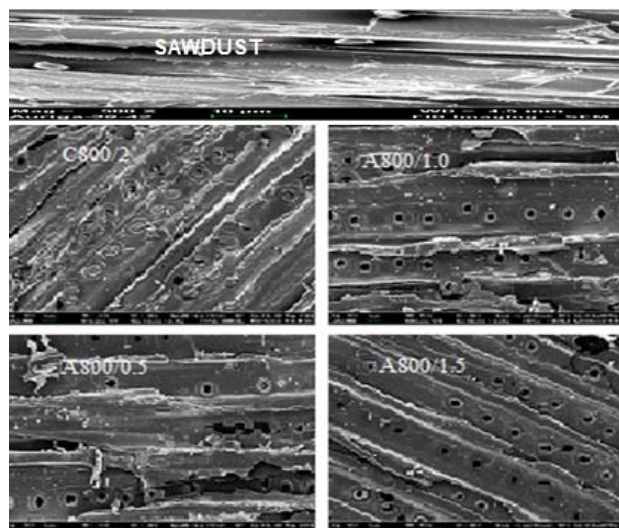

Fig. 5 SEM micrographs of sawdust, C800/2 chars and AC samples (A800/0.5, A800/1.0 and A800/1.5): -1000 + 850μm; Mag. = 500 X 10μm

D. Activated Carbon Surface Functionalities

The proton binding isotherms of the developed AC (A800/1.5) and sawdust were shown in Fig. 6. The isotherm(s) was generated using an indefferent background electrolyte (NaCl) and, therefore, the isotherm curve was due to surface protonation i.e. binding/consumption of solution protons by sample basic surface groups, and as well as deprotonation i.e. proton release by surface acidic groups into solution [26]. The developed AC pHPZC i.e. solution pH at which the net proton transfer to surface is zero was estimated at 10.3, indicative of highly basic characteristics. The pHPZC is a property of the AC and its determination is important in evaluation of AC surface charge with respect to solution pH. The aqueous phase ionization characeristics of AC surface functional groups determine the type of AC surface charge. In turn, the AC surface charge and speciation of the solute in water determine the nature of interaction forces between the two e.g. elecrostatic interaction. The developed AC determined pHPZC of 10.3 indicated that the AC would assume positive surface charge for solution pH < 10.3 and vice vesa for solution pH > 10.3. By comparison, the sawdust pH$_{PZC}$ was estimated at 5.5 (insert in Fig. 6), indicative of relatively high acidic surface functionalities.Therefore, the sawdust carbonization/activation conditions developed a highly basic AC that would preferentially adsorb aqueous anionic species for solution pH < 10.3.

World Academy of Science, Engineering and Technology
International Journal of Chemical and Molecular Engineering
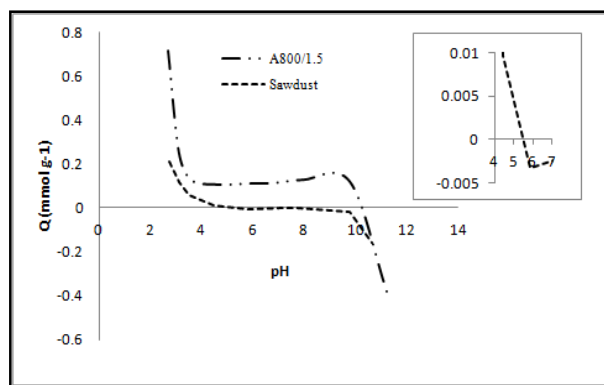Vol:7, No:7, 2013

Fig. 6 Proton binding isotherm @ 25°C for sawdust and developed AC (A800/1.5)

The total acidity and basicity of the developed AC was quantified by the Boehm titration and results included in Table VI. The developed AC total acidity and basicity were measured at 944mmol/g and 62µmol/g respectively, while sawdust total acidicity and basicity were measured at 824 and 117µmol/g rsepectively. The aqueous suspension pH could provide an indication of the type of surface groups on carbon samples. The aqueous suspension pH of the developed AC was measured at 10.2. An alkaline AC aqueous suspension pH was indicative of protonation of the AC basic surface groups and hence, excess OH^- ions in solution. These results are consistent with conclusions drawn from the proton binding isotherm(s).

TABLE VI
ACID-BASE NEUTRALIZATION CAPACITIES OF DEVELOPED AC (A800/1.5)
AND SAWDUST

Sample	T_A (µmol/g)	T_B (µmol/g)	pH*	pH_{PZC}
A800/1.5	62.5	944.44	10.2	10.3
Sawdust	823.67	116.67	4.5	6

*aqueous suspension pH; T_A: total acidity; T_B: total basicity

The AC surface functional groups are mainly carbon-oxygen surface complexes [26]. Acidic carbon-oxygen surface groups are well characterized and include carboxylic, lactonic and phenolic groups. Basic surface groups are postulated as a contribution of carbon-oxygen surface groups (carbonyl, pyrone and chromene) and Lewis sites (i.e. delocalised π-electrons system at basal graphene planes). The information on the chemical nature of surface functional groups on developed AC (A800/1.5) was obtained from FTIR spectrographs and results presented in Fig. 7. The FTIR spectra were provided for evaluation of presence or absence of acidic carbon-oxygen surface groups particular to ACs in the fingerprint (900 - 1300cm^{-1}) and broad (3200 - 3600cm^{-1}) IR spectral regions [27]. The transmission intensities in the the fingerprint IR regions are peculiar to oxidized carbons and ascribable to C-O bending vibrations in carboxylics, phenols, alcohols, esters and ethers: Intensities in the broad IR region are ascribable to hydroxyl stretch vibration in carboxylic, phenolic and lactonic groups. An unambiguous assignment of vibrational intensities of AC basic oxygen suface groups is difficult with IR analysis. Accordingly, the sawdust showed weak broad transmission intensty of minimun 1030cm^{-1} in the fingerprint band (800-1200cm^{-1}), and very weak broad intensity at 3300cm^{-1} in the broad band (3100-3600cm^{-1}). On the other hand, the AC(A800/1.5) spectrum showed minimal vibrational intensities in the considered IR spectral bands. The absence or minimal transmission intensities in both the fingerprint and broad IR spectral regions was indicative of very low concentrations of acidic carbon-oxygen surface groups of the type carboxylic, lactonic, phenolic, etc. on the developed AC. The FTIR result complemented the results of the Boehm titration. The nature and amounts of AC oxygen surface groups depend on the chemical nature of precursor material, oxidizing agent and activation conditions. The highly basic nature of the developed AC could be attributed to the thermal decomposition of most acidic carbon-oxygen surface groups at the activation conditions of 800°C, and thereby, leaving the AC surface with high basic functionalitie [28].
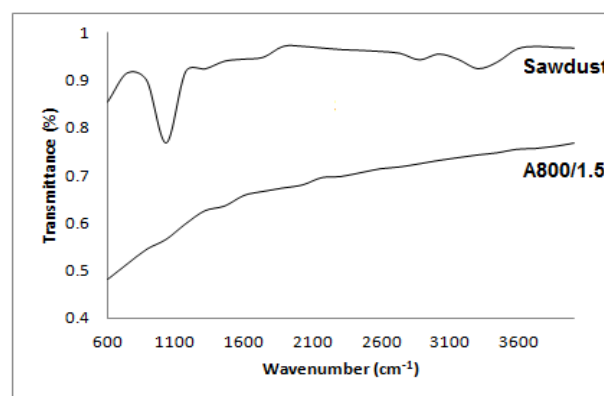

Fig. 7 FTIR spectrographs of (*Pinus patula*) sawdust and derived AC (A800/1.5) by two-stage N_2-steam activation at 800°C and 1.5hrs

E. Comparison of Textural Properties

A comparison of textural properties of the developed AC of this study with literature sawdust derived low-cost ACs and commercial ACs was made and results presented in Table VII, Appendix. The surface area (1086m^2/g) of the developed AC of this study was comparable to most commercial ACs, and higher than most sawdust derived ACs. The majority of high surface area (>900m^2/g) sawdust derived ACs were developed by the relatively expensive chemical activation method (cf. steam activation) and were mostly microporous. The sawdust derived AC of this study showed high [wide] microporosity and mesoporosity distribution significant to increased adsorption capacity and fast adsorption kinetics of water solutes of rather large molecular/ionic sizes [18], [25]. These results identified the South Africa pine tree (*Pinus patula*) sawdust as a suitable precursor for development of better quality AC by the superheated steam activation in a fixed-bed reactor.

F. Comparative Phenol Equilibrium Adsorption

The comparative equilibrium adsorption was conducted for purpose of comparing the adsorption capacities of the developed AC (A800/1.5) with commercial AC (Norit RO

World Academy of Science, Engineering and Technology
International Journal of Chemical and Molecular Engineering
Vol:7, No:7, 2013

0.8) for phenol removal from aqueous solution. The Norit AC (RO 0.8) was selected on the basis of vendor quality specification being similar to developed AC (A800/1.5) evaluated quality. Accordingly the Norit AC (RO 0.8) is specified as a basic AC (S_{BET} = 1200m^2/g) suitable for wastewater/water purification. Prior to generation of phenol equilibrium adsorption data for the ACs, experiments were conducted for selection of optimum aqueous solution pH for maximum phenol uptake on the developed AC, and results presented in Fig. 8.
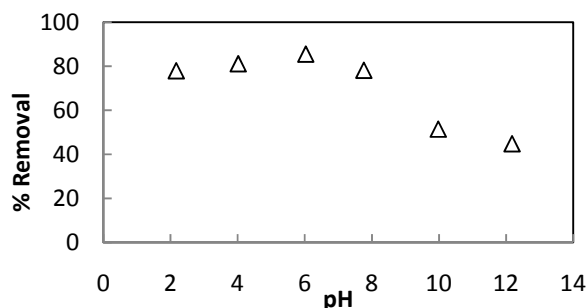

Fig. 8 Effect of solution pH on equilibrium adsorption of phenol onto developed AC: 100mg/l; 298K; 25ml; 0.8g/l AC; 24hrs; 200rpm; -300+150μm

The developed AC phenol percent removal peaked with increase of solution pH. The phenol percent removal increased (ca. 78 - 85%) for increase of solution pH 2 - 6, and for pH increase 6 - 12 the percent removal decreased (ca. 85 - 45%). At the solution pH < 9.89 phenol is in unionized state (pKa = 9.89), and for solution pH < 10.3 the AC surface is positvely charged (pH$_{PZC}$ =10.3). The adsorption of unionied phenol on positive AC surface could be attributed to dispersive π-π interactions and electron donor-acceptor complexes formation [26]. At very low pH the high protation of AC surface would shield the phenol ring from accessing the basal π-electrons system and thereby relatively reduced phenol adsorption. For very high pH the low phenol adsorption could be attributed to coulombic repulsion between increased phenolate ions and negative charged AC surface. In this study, solution pH 6.0 was taken as the optimum for generation of phenol adsorption isotherm data for the developed AC and Norit AC, and results presented in Figs. 9 and 10 respectively.

TABLE VII
COMPARISON OF TEXTURAL PROPERTIES OF DEVELOPED AC WITH LITERATURE SAWDUST DERIVED LOW-COST AND COMMERCIAL ACS

Precursor (AM)	S_{BET} (m^2/g)	V_T (cm^3/g)	V_{mic} (cm^{3}g^{-1})	Ref.
H. braziliensis SAC (CA/PA)	686	0.70	0.27	[29]
P. aculeate SAC-A (CA)	968	0.70	0.18	[30]
CAC	1424	1.08	0.28	[30]
P. ruscifolia SAC (CA)	1638	1.30	0.92	[31]
CAC	1152	0.60	0.59	[31]
Rattan SAC (CA/PA)	1083	0.64	-	[32]
Fly ash SAC (PA)	613	0.49	0.27	[33]
CAC	924	0.47	0.43	[33]
Eucalyptus SAC (PA)	367	0.99	0.55	[34]
H. courbaril SAC (PA)	1003	0.54	0.46	[35]
CAC	627	0.39	0.22	[36]
Chegal SAC (CA)	1496	0.86	0.47	[37]
Rubber wood SAC (PA)	684	0.47	0.37	[38]
Pine wood SAC (CA)	593	0.28	0.18	[39]
Pine wood SAC (PA)	796	0.39	0.26	[39]
CAC	1057	0.58	0.39	[39]
P. patula SAC (PA)	1086	0.69	0.26	This study

AM: activation method; SAC: sawdust activated carbon; CAC: commercial activated carbon; PA: physical activation; CA: chemical activation
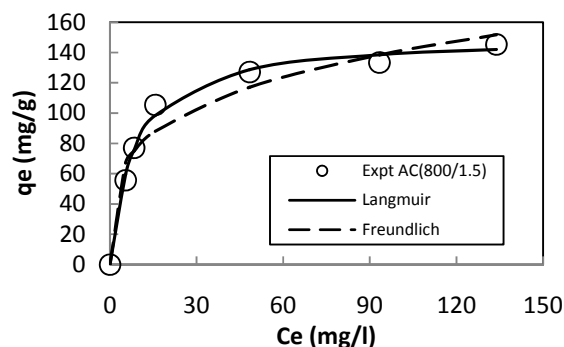

Fig. 9 Adsorption isotherm at 298K for sorption of phenol on developed AC: pH 6.0±0.3; 25ml; 0.8g/l AC; 24hrs; 200rpm; -300+150μm; Co: 50-250mg/l
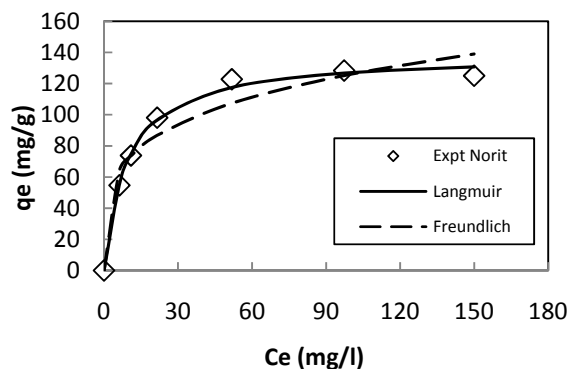

Fig. 10 Adsorption isotherm at 298K for sorption of phenol on Norit (RO 0.8) AC: pH 6.0±0.2; 25ml; 0.8g/l AC; 24hrs; 200rpm; -300+150μm; Co: 50-250mg/l

The experimental isotherms were calibrated with the Langmuir (refer to (1)) and Freundlich (refer to (2)) isotherm models. The applicability of model to isotherm data was validated by non-linear regression of minimizing the stastical error function of the Chi-squared (χ^2) test [17]:

World Academy of Science, Engineering and Technology
International Journal of Chemical and Molecular Engineering
Vol:7, No:7, 2013

$$\chi^2 = [(q_e \exp - q_e cal)^2 / q_e \exp] \qquad (10)$$

The solutions to the Chi-squared test were generated using Microsoft Excell 2007, Add-in solver, and results presented in Table VII.

TABLE VIII
$25^{\circ}C$ ISOTHERM MODEL PARAMETERS FOR PHENOL ADSORPTION ONTO A800/1.5 AND NORIT ACTIVATED CARBONS

Model	Activated carbon type	
	A800/1.5	Norit (RO 0.8)
Langmuir	Q_{max} = 150.92 mg/g	Q_{max} = 139.00 mg/g
	K_L = 0.12 L/mg	K_L = 0.11 L/mg
	$0 < R_L < 1$ ($C_O > 0$)	$0 < R_L < 1$ ($C_O > 0$)
	$\chi2$ = 1.08	$\chi2$ = 0.54
Freundlich	K_F = 43.66 mg/g	K_F = 41.14 mg/g
	Fr = 3.93	Fr = 4.12
	$\chi2$ = 6.65	$\chi2$ = 6.58

The results in Table VIII indicated that the adsorption isotherm data for both AC systems were better fitted by the Langmiur model (lowest $\chi2$ values), suggestive of homogeneous monolayer adsorption mechanism. The K_L values and thus the dimensionless separation factor, R_L values were similar. The range $0 < R_L < 1$ was indicative of favorable phenol adsorption on both ACs [17]. However, the phenol equilibrium monolayer uptake by the developed AC of 151mg/g was higher than that by Norit AC of 139mg/g. The comparative phenol equilibrium adsorption capacities were extended to include literature ACs, and results presented in Table IX. The results indicated that the aqueous phase adsorption capacity of the developed AC for phenol was on the high side. The significant aspect of this study is that AC was developed from cheap and locally available sawdust resource material, and therefore, it could be used for efficient and economical treatment of phenol polluted wastewaters at reduced costs.

TABLE IX
COMPARISON OF LITERATURE ACTIVATED CARBONS MAXIMUM ADSORPTION CAPACITIES FOR PHENOL

Activated carbon type	Q_{max} (mg/g)	Reference
Bugasse fly ash (BFA)	23.83	[40]
CAC	30.22	[40]
Laboratory AC	24.64	[40]
CAC	49.72	[41]
Cork oak AC	187.28	[42]
Coconut shell AC	47	[43]
Rattan SAC	149.25	[32]
CAC	165.50	[44]
Coir Pitch AC	43.29	[45]
Oil palm EFB AC	4.87	[46]
CAC	238.09	[47]
T. grandis SAC	13.45	[48]
Pine wood SAC	10.00	[39]
P.paluta sawdust AC	151	This study
CAC (Norit RO 0.8)	139	This study

CAC: commercial AC; SAC: sawdust AC

IV. CONCLUSION

This study demonstrated the capacity to develop better quality low-cost AC from SA cheap and abundantly available pine tree (*Pinus patula*) sawdust using the two-stage N_2-superheated steam activation in a fixed-bed reactor. Relatively low slow pyrolysis activation energy was required to pyrolyze the sawdust. The slow pyrolysis activation energy of the sawdust was estimated at $131kJ/mol^2$. The textural properties of the developed low-cost AC are highly competitive to literature commercial ACs and exceeds majority of literature biomass waste derived low-cost AC. The results of this study also indicated that at aqueous solution pH 6, the Langmuir adsorption capacity of the developed AC for phenol was higher than that of commercial AC (Norit RO 0.8) and majority of literature sawdust derived low-cost ACs.

REFERENCES

[1] U. Pruss-Ustun, R. Bos, F. Gore, J. Bartram, 2008. "Safer water, better health: Costs, benefits and sustainability of interventions to protect and promote health," World Health Organisation, Geneva, 2008.
[2] H. Zhou, D. W. Smith, "Advanced technologies in water and wastewater treatment," *J. Environ. Eng. Sci.* vol.1, pp. 247–264, 2002.
[3] N. Bolong, A. F. Ismail, M. R. Salim, T. Matsuura, "_A review of the effects of emerging contaminants in wastewater and options for their removal," *Desalination* 239, pp. 229–246, Mar. 2009.
[4] D. Rhedditota, A.Yerramilli, R. J. Krupadam, "Electrocoagulation: A cleaner method for treatment of Cr (VI) from electroplating industrial effluents," *Indian journal of chemical technology,* vol. 14, pp. 240-245, May 2007.
[5] R. Qu, J. Shi, D. Li, Z. Wei, X. Yang, Z. Wang, "Heavy Metal and Phosphorus Removal from Waters by Optimizing Use of Calcium Hydroxide and Risk Assessment," *Environment and Pollution*, vol. 1, no.1, pp. 38-54, Jan. 2012
[6] P. C. Mouli, S. K. Mohan, J. S. Reddy, "Electrochemical processes for the remediation of waste water and contaminated soil: emerging technology," *Journal of scientific and industrial research,* vol. 63, pp. 11-19, Jan. 2004.
[7] A. Rubalcaba, M. E. Suarez-Ojeda, F Stuber, A. Fortuny, C. Bengoa, I. Metcalfe, J. Font, J. Carrera, A. Fabregat, "Phenol wastewater remediation: advanced oxidation processes coupled to a biological treatment," *Water Science & Technology*, vol. 55, no. 12, pp. 221–227, 2007.
[8] A. Ahmad, M. Rafatullahb, O. Sulaimanb, M. H. Ibrahima, Y. Y. Chiia, B. M. Siddiquea, "Removal of Cu (II) and Pb (II) ions from aqueous solutions by adsorption on sawdust of Meranti wood," *Desalination,* 247, pp. 636–646, Jan. 2009.
[9] N. S. Mamphweli, E. L. Meyer, "Implementation of the biomass gasification project for community empowerment at Melani village, Eastern Cape, South Africa," *Renewable Energy* 34, pp. 2923–2927, Jun. 2009.
[10] D. Honsbein, "Examples of Biomass Utilisation in South Africa – PyNe issue 21," 2009 [Online]. Available from: http://www.pyne.co.uk/Resources/user/PYNE%20Newsletters/PyNews %2021.pdf [Accessed: 2010/11/23].
[11] G. Busca, S. Berardinelli, C. Resini, L. Arrighi, "Technologies for the removal of phenol from fluid streams: A short review of recent

World Academy of Science, Engineering and Technology
International Journal of Chemical and Molecular Engineering
Vol:7, No:7, 2013

developments," *Journal of Hazardous Materials* 160, pp. 265–288, 2008.

[12] K. Acikalm, "Pyrolytic characteristics and kinetics of pistachio shell by thermogravimetric analysis," *J. Therm. Anal.Calori,* May 2011.

[13] K. B. Cantrell, J. H. Martin, K. S. Ro, "Application of Thermogravimetric Analysis for the Proximate Analysis of Livestock Wastes," *Journal of ASTM International*, Vol. 7, No. 3, pp. 1-13, Jan. 2010.

[14] M. Valix, W. H. Cheung, G. McKay, "Preparation of activated carbon using low temperature carbonisation and physical activation of high ash raw bagasse for acid dye adsorption," *Chemosphere* 56, pp. 493–501, Apr. 2004.

[15] S. L. Goertzen, K. D. Theriault, A. M. Oickle, A. C. Tarasuk, H. A. Andreas, "Standardization of the Boehm titration. Part I. CO_2 expulsion and endpoint determination," *Carbon* 48, pp. 1252-1261, 2010.

[16] A. M. Puziy, O. I. Poddubnaya, V. N. Zaotsev, O. P. Konoplitska, "Modelling of heavy metal ion binding by phosphoric acid activated carbons," *Applied Surface Science* 221, pp. 421- 429, Jul. 2004.

[17] K. Foo, B. H. Hameed, "Insight into the modeling of adsorption isotherm systems," *Chemical Engineering journal* 156, pp. 2-10, 2010.

[18] H. Marsh, R. F. Rodriguez, *Activated carbon*, 1st ed. United Kingdom: *Elsevier Ltd*. 2006, pp. 13-86, 143-365.

[19] J. E. White, W. J. Catallo, B. L. Legendre, "Biomass pyrolysis kinetics: A comparative critical review with relevant agricultural residue case studies," *Journal of Analytical and Applied Pyrolysis* 91, pp. 1–33, 2011.

[20] M. Guerrero, M. P. Ruiz, M. U. Alzueta, R. Bilbao , A. Millera, "Pyrolysis of eucalyptus at different heating rates: studies of char characterization and oxidative reactivity," *J. Anal. Appl. Pyrolysis* 74, pp. 307–314, Mar. 2005.

[21] S. H. Beis, O. Onay, O. M. Kockar, "Fixed-bed pyrolysis of safflower seed: influence of pyrolysis parameters on product yields and compositions," *Renewable Energy* 26, pp. 21–32, 2002.

[22] S. Baral, S. N. Das, P. Rath, "Hexavalent chromium removal from aqueous solution by adsorption on treated sawdust," *Biochemical Engineering Journal* 31, pp. 216–222, Aug. 2006.

[23] N. Tancredi, T. Cordero, J. R. Mirasol, J. J. Rodriguez, "Activated carbons from Uruguayan eucalyptus wood," *Fuel*. vol. 75, no. 15, pp. 1701-1706, 1996.

[24] T. Yang, A. C. Lua, Characteristics of activated carbons prepared from pistachio-nut shells by physical activation. *Journal of Colloid and Interface Science* 267, pp. 408–417, Jul. 2003.

[25] C. T. Hsieh, H. Teng, "Influence of mesopore volume and adsorbate size on adsorption capacities of activated carbons in aqueous solutions," *Carbon* 38, pp. 863–869, 2000.

[26] C. Moreno-Castilla, "Adsorption of organic molecules from aqueous solutions on carbon Materials," *Carbon* 42, pp. 83–94. 2004

[27] A. M. Puziy, O. I. Poddubnaya, A. M. Alonso, A. C. Muniz, F. S. Garcıa, J. S. J. Tascon, " Oxygen and phosphorus enriched carbons from lignocellulosic material," *Carbon* 45, pp. 1941–1950, Jul. 2007.

[28] F. Villacanas, M. F. R. Pereira, J. J. M. Orfao, J. L, Figueiredo, "Adsorption of simple aromatic compounds on activated carbons," *Journal of Colloid and Interface Science* 293, pp. 128–136, 2006.

[29] K. A. Krishnan, K. G. Sreejalekshmi, S. Varghese, "Adsorptive retention of citric acid onto activated carbon prepared from Havea braziliansis sawdust: Kinetic and isotherm overview," *Desalination* 257, pp. 46–52, 2010.

[30] G. V. Nunell, M. E. Fernandez,P. E. Bonelli, A. L. Cukierman, "Conversion of biomass from an invasive species into activated carbons for removal of nitrate from wastewater," *Biomass and bioenergy 44*, pp. 87-95, 2012.

[31] D. Nabarlatz, J. De Celis, P. Bonelli, A. L. Cukierman, " Batch and dynamic sorption of Ni (II) ions by activated carbon based on a native lignocellulosic precursor," *Journal of Environmental Management* 97, pp. 109-115, 2012.

[32] B. H. Hameed, A. A. Rahman, "Removal of phenol from aqueous solutions by adsorption onto activated carbon prepared from biomass material," *Journal of Hazardous Materials* 160, pp. 576–581, 2008.

[33] A. Aworn, P. Thiravetyan, W. Nakbanpote, "Preparation and characteristics of agricultural waste activated carbon by physical activation having micro- and mesopores," *J. Anal. Appl. Pyrolysis* 82, pp. 279–285, 2008.

[34] L. Giraldo- Gutierrez, J. C. Moreno- Pirajan, " Pb(II) and Cr(VI) adsorption from aqueous solution on activated carbons obtained from

sugar cane husk and sawdust," *J. Anal. Appl. Pyrolysis* 81, pp. 278–284, Jan. 2008

[35] J. Matos, C. Nahas, L. Rojas, M. Rosales, "Synthesis and characterization of activated carbon from sawdust of Algarroba wood. 1. Physical activation and pyrolysis," *Journal of Hazardous Materials* 196, pp. 360– 369, 2011.

[36] S. Noonpui, P. Thiravetyan, W. Nakbanpote, S. Netpradit, "Color removal from water-based ink wastewater by bagasse fly ash, sawdust fly ash and activated carbon," *Chemical Engineering Journal* 162, pp. 503-508, May 2010.

[37] K. Y. Foo, B. H. Hameed, "Mesoporous activated carbon from wood sawdust by K_2CO_3 activation using microwave heating," *Bioresource Technology* 111, pp. 425–432, 2012.

[38] E. Taer, M. Deraman, I. A. Talib, A. A. Umar, M. Oyama, R. M. Yunus, "Physical, electrochemical and super capacitive properties of activated carbon pellets from pre-carbonized rubber wood sawdust by CO2 activation," *Current Applied Physics* 10, pp. 1071–1075, 2010.

[39] E. T. Musapatika " Use of low-cost adsorbents to treat industrial wastewater," MSc. Eng. Johannesburg, University of the Witwaterand, 2010.

[40] V. C. Strivastava, M. M. Swamy, I. D. Mall, B. Prasad, I. M. Mishra, "Adsorptive removal of phenol by bagasse fly ash and activated carbon: equilibrium, kinetics and thermodynamics," *Colloids Surf. A: Physicochem. Eng. Aspects* 272, pp. 89–104, Sept. 2006.

[41] B. Ozkaya, "Adsorption and desorption of phenol on activated carbon and a comparison of isotherm models," *Journal of Hazardous Materials,* B129, pp. 158–163, 2006.

[42] P. A. M. Mourao, P. J. M. Carrott, M. M. L. R. Carrott, "Application of different equations to adsorption isotherms of phenolic compounds on activated carbons prepared from cork," *Carbon* 44, pp. 2422–2429, May 2006.

[43] K. P. Singh, A. Malik, S. Sinha, P. Ojha, "Liquid phase adsorption of phenol using activated carbons derived from agricultural waste material," *Journal of Hazardous Materials* 150, pp. 626-641, 2008.

[44] A. Kumar, S. Kumar, S. Kumar, D. V. Gupta, "Adsorption of phenol and 4-nitrophenol on granular activated carbon in basal salt medium: equilibrium and kinetics," *J. Hazard. Material* 147, pp. 155–166, Dec. 2007.

[45] T. S. Anirudhan, S. S. Sreekumari, C. D. Bringle, **"**Removal of phenols from water and petroleum industry refinery effluents by activated carbon obtained from coconut coir pith," *Adsorption* 15, pp. 439–451, Aug. 2009.

[46] Z. Alam, E. S. Ameem, S. A. Muyibi, N. A. Kabbashi, "The factors affecting the performance of activated carbon prepared from oil palm empty fruit bunches for adsorption of phenol," *Chemical Engineering Journal* 155, pp. 191-198, 2009.

[47] O. Hamdaoui, E. Naffrechoux, "Modeling of adsorption isotherms of phenol and chlorophenols onto granular activated carbon Part I. Two-parameter models and equations allowing determination of thermodynamic parameters," *Journal of Hazardous Materials* 147, pp. 381–394, Jan. 2007.

[48] K. Mohanty, D. Das, M.N. Biswas, "Adsorption of phenol from aqueous solutions using activated carbons prepared from *Tectona grandis* sawdust by ZnCl2 activation," *Chemical Engineering Journal* 115, pp. 121–131, Sept. 2005.